Supplement of Earth Syst. Sci. Data, 17, 3089–3108, 2025
https://doi.org/10.5194/essd-17-3089-2025-supplement

Open Access Earth System Science Data

Supplement of

A high-quality data set for seismological studies in the East Anatolian Fault Zone, Türkiye

Leonardo Colavitti et al.

Correspondence to: Leonardo Colavitti (leonardo.colavitti@edu.unige.it)

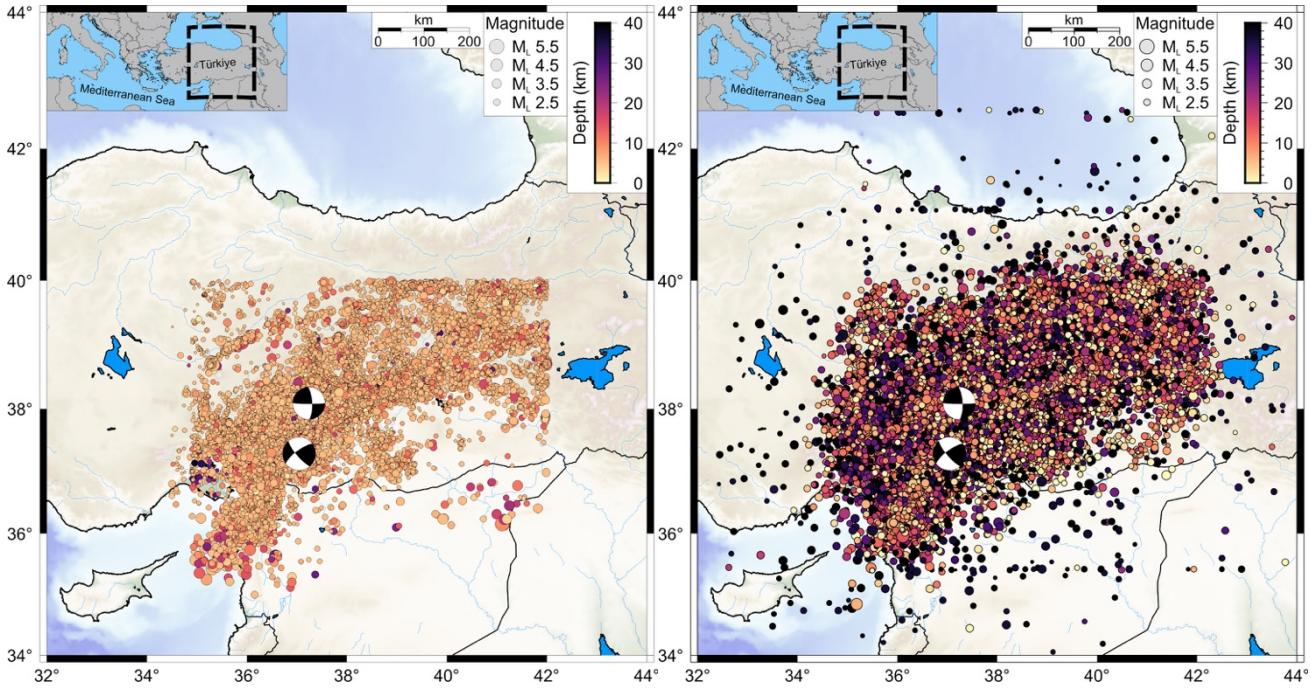

Figure S1: Selected events from the initial reference catalog with any value of magnitude in the time period from 01-01-2019 to 29-02-2024. On the left location given by AFAD, on the right location in this work. Size is proportional to the magnitude, color palette shows the event depth.

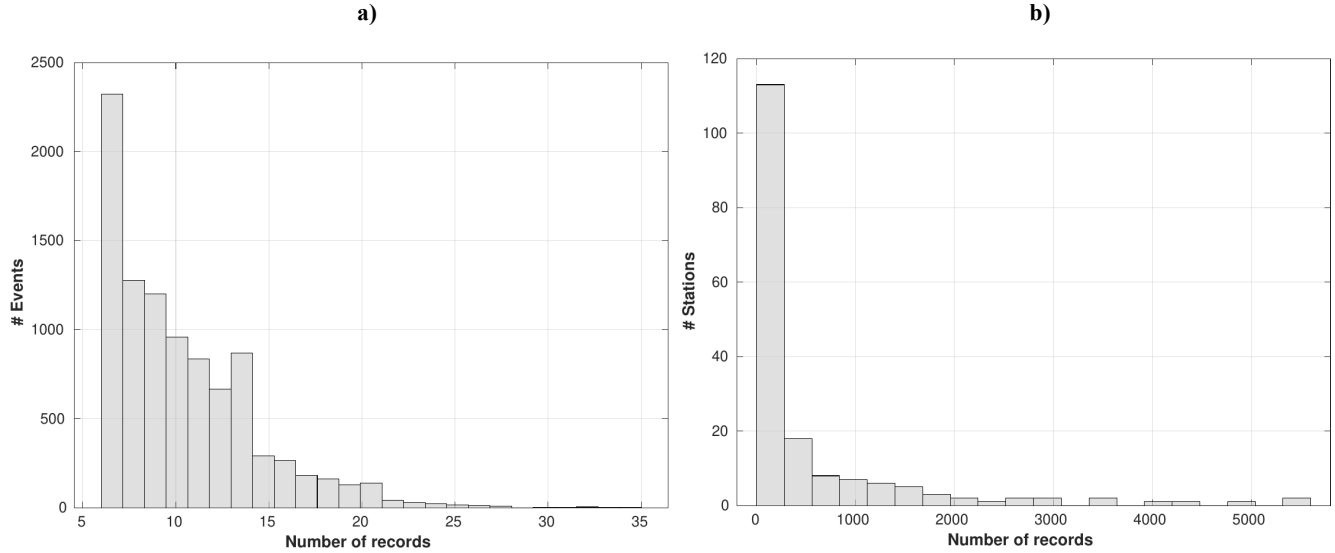

Figure S2: Number of records per event (a) and per stations (b) used in this product.

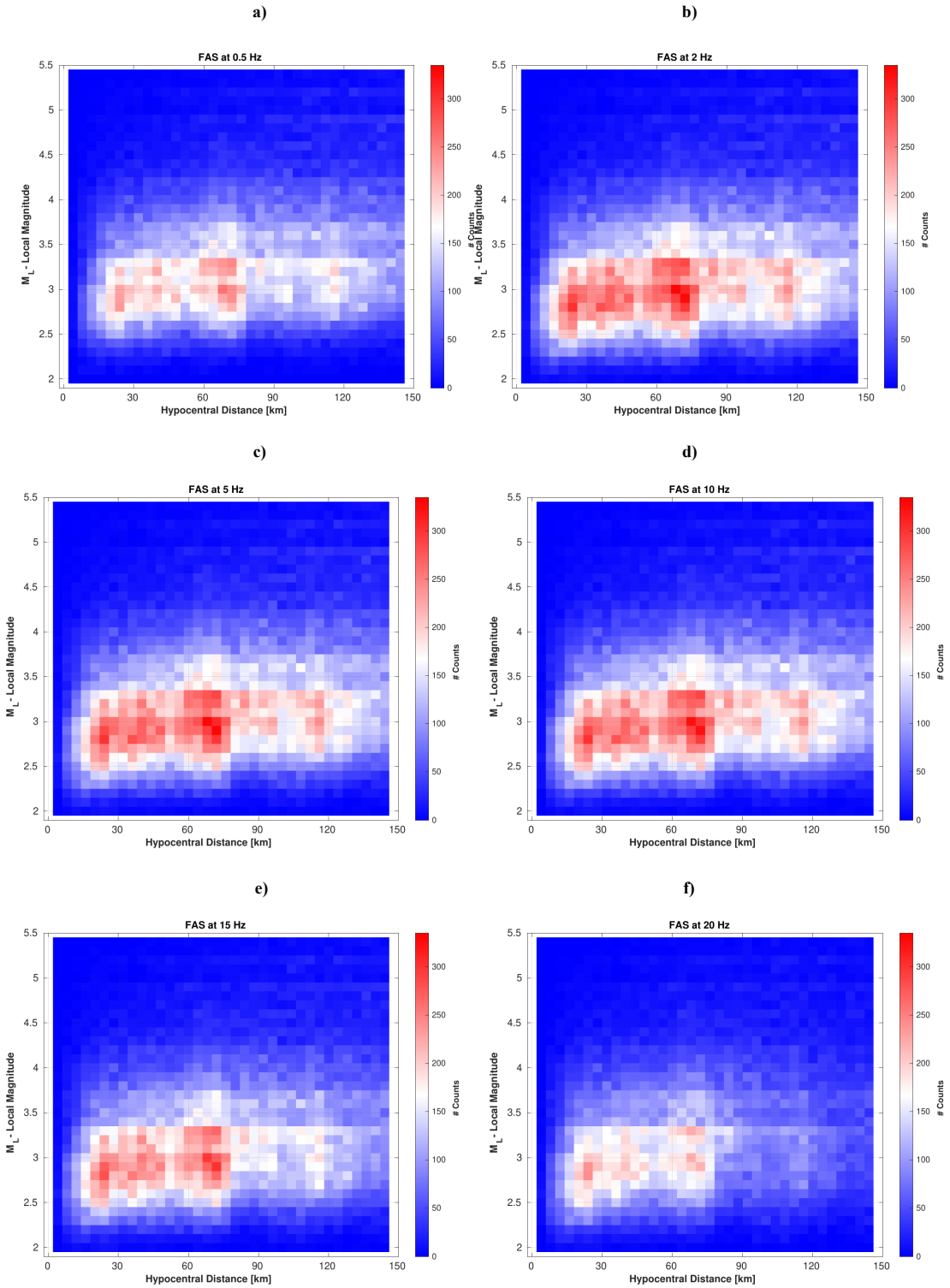

Figure S3: Hypocentral distance vs M_L at different frequencies for FAS at a) 0.5 Hz; b) 2 Hz; c) 5 Hz; d) 10 Hz; e) 15 Hz; f) 20 Hz.

a)

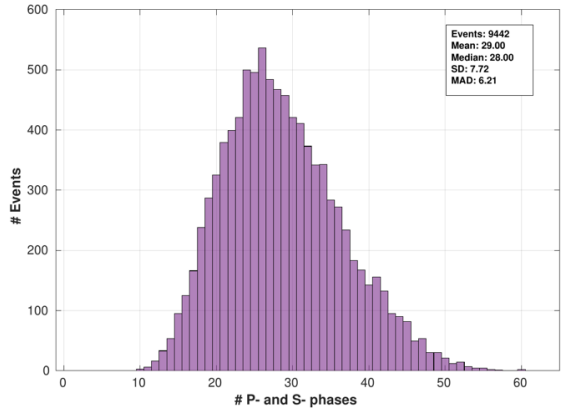

b)

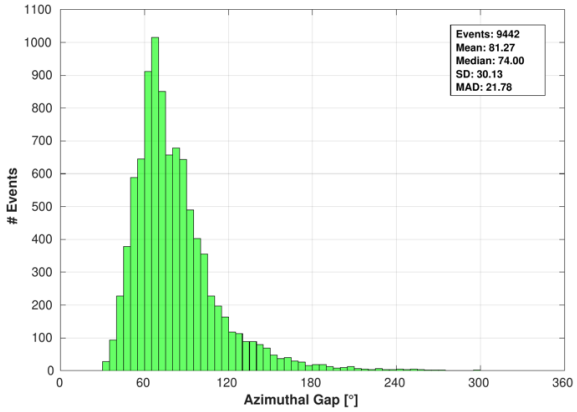

c)

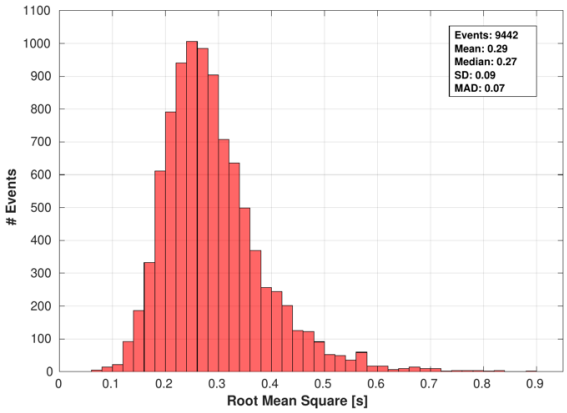

Figure S4: a) Histogram of number of total phases (P and S) picked by the Complete Automatic Seismic Processor procedure (CASP); b) azimuthal gap (in degrees) for each event of the data set; c) root mean square error (in seconds) for each event of the data set.

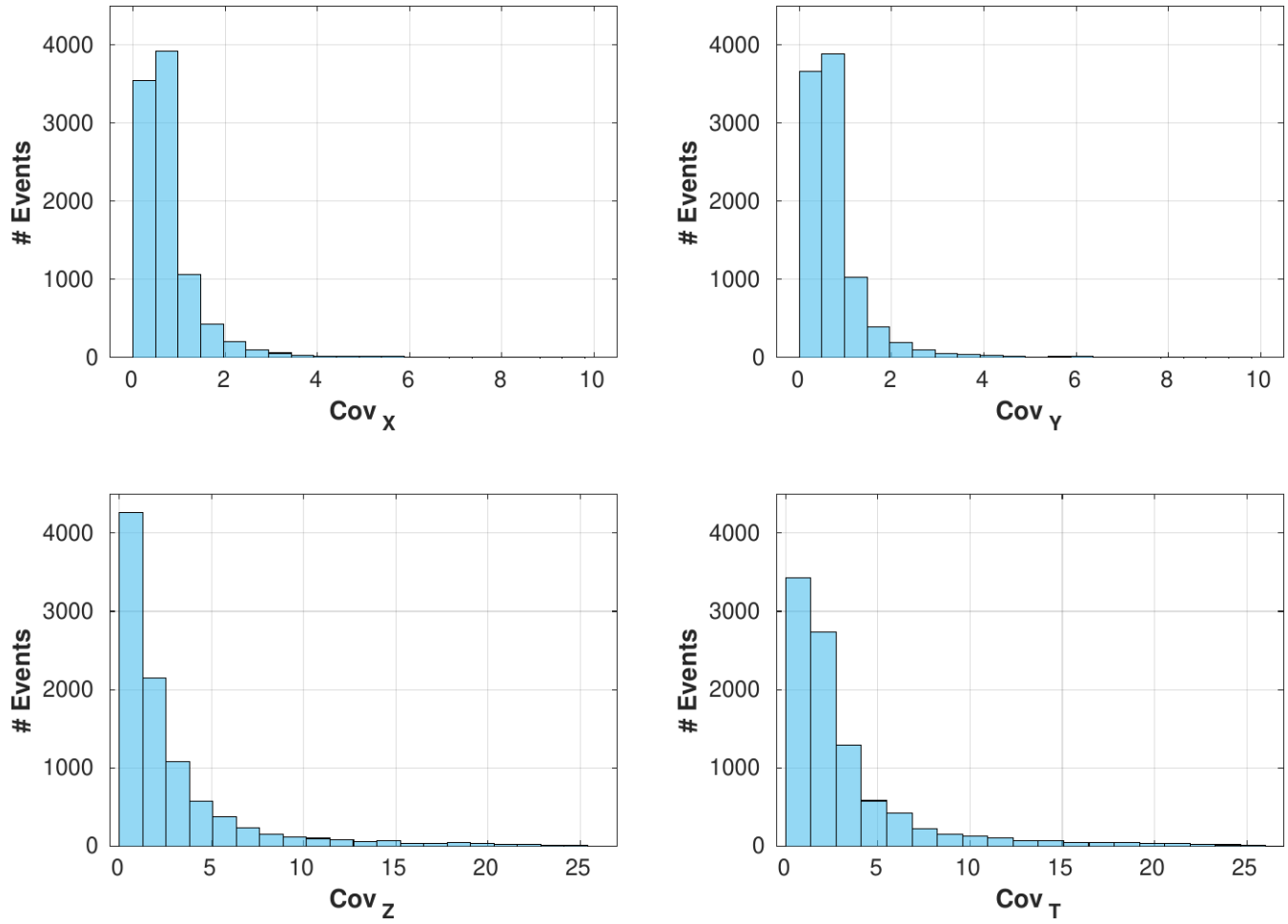

Figure S5: Distribution of covariance matrices for the events analyzed in this dataset. Top left Cov_x, top right Cov_y, bottom left Cov_z and bottom right Cov_T.

a)

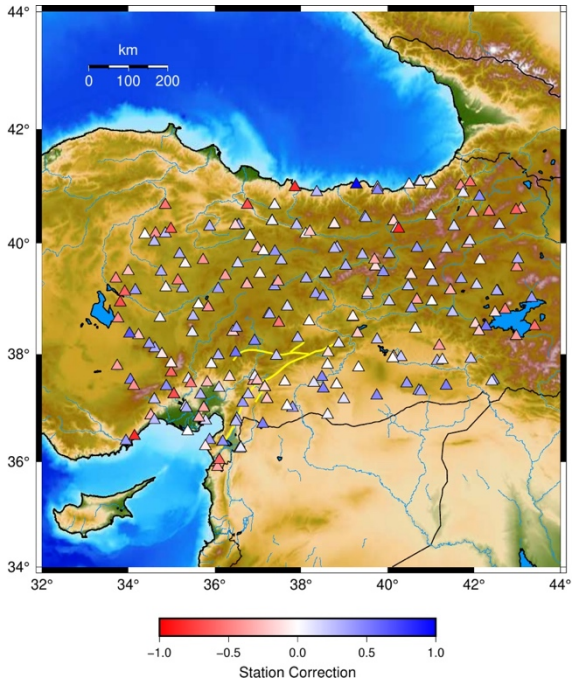

b)

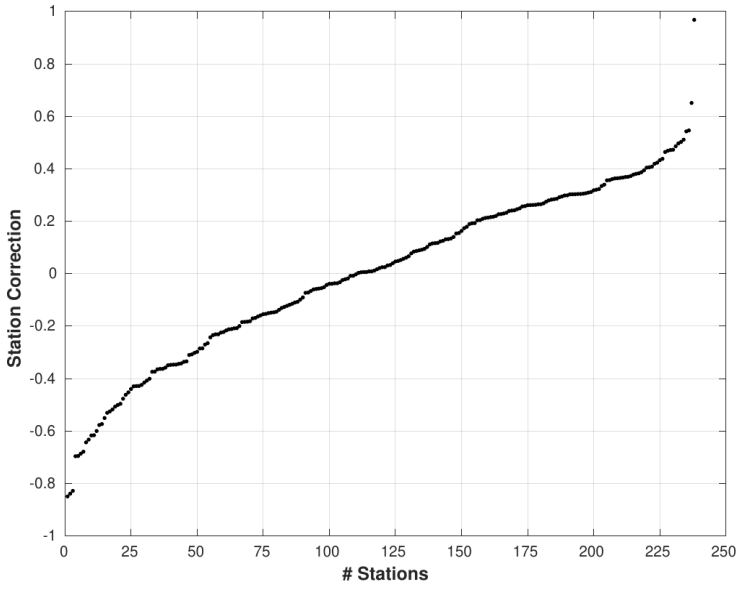

Figure S6: Station correction obtained in this study presented in map a) and in the graph b).

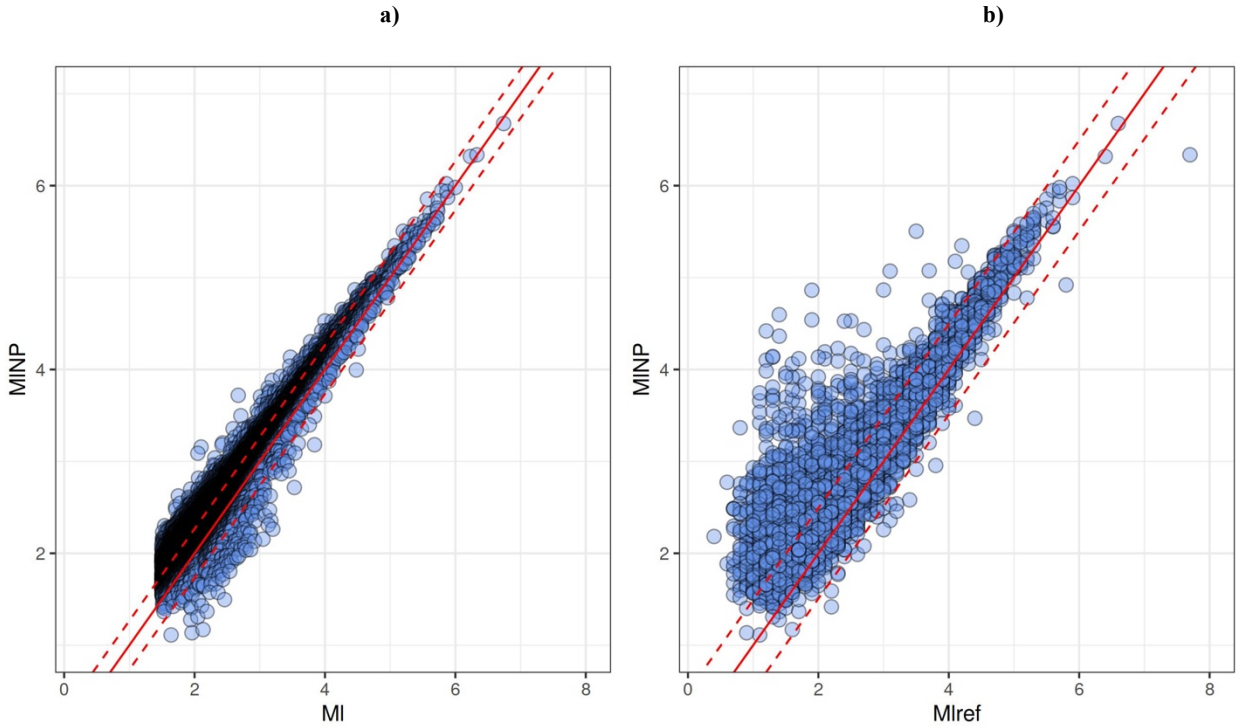

Figure S7: Comparison between non parametric magnitude (MNP) with recomputed local magnitude M_L (a) and local magnitude from AFAD catalogue (b). Dashed lines correspond to the line 1:1 shifted by $\pm$ 2 standard deviations of the residuals between the reported magnitudes. Value of 1 Standard deviation: a) 0.13; b) 0.25.

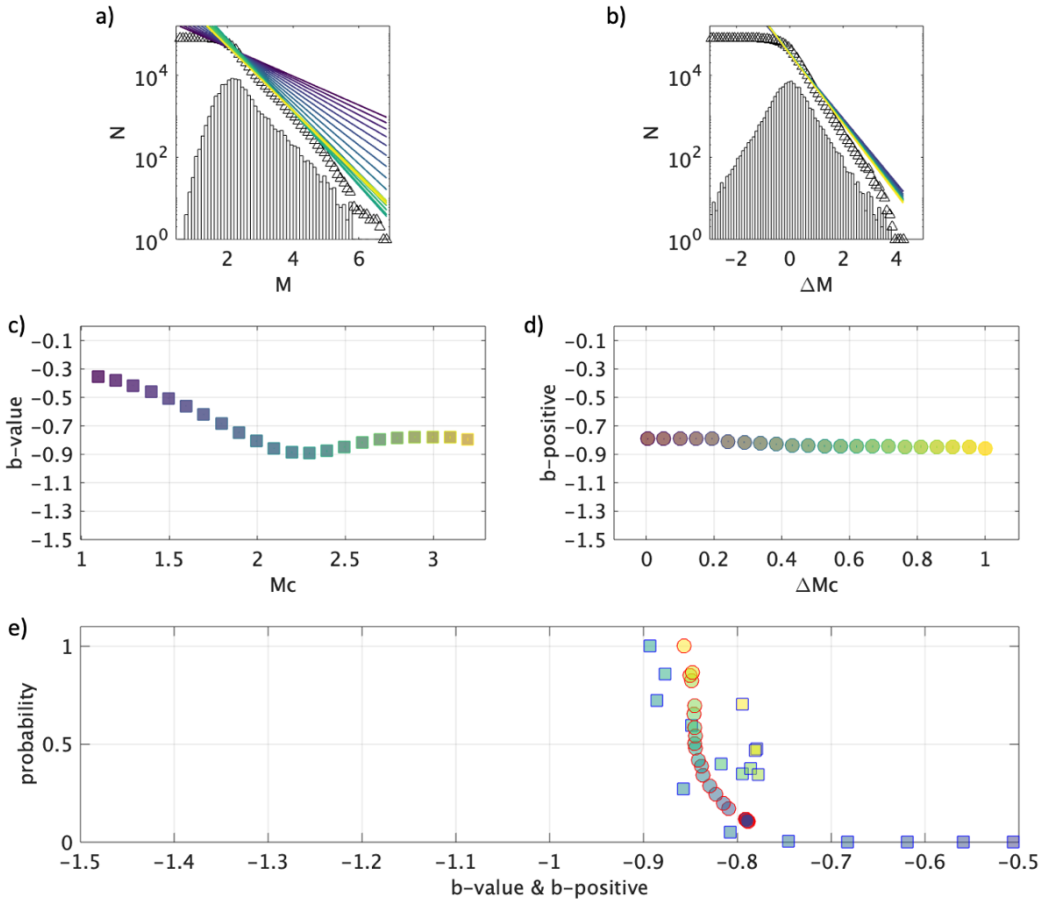

Figure S8: a) Cumulative frequency magnitude distribution for the ALL dataset and the Gutenberg-Richter law colored for different low magnitude cutoff.
b) The same as a), but for b-positive.
c) b-value estimates for different low magnitude cutoff.
d) The same as c), but for b-positive.
e) Probability of b-value and b-positive estimates.

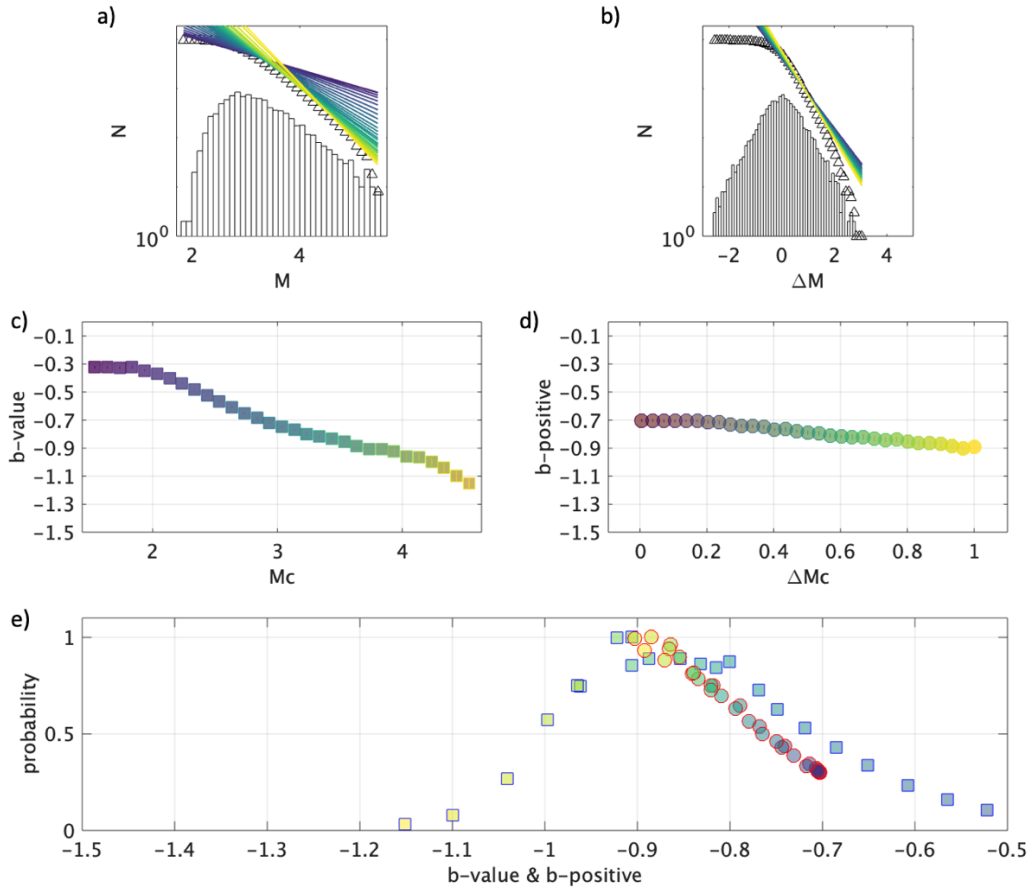

Figure S9: a) Cumulative frequency magnitude distribution for the GIT dataset and the Gutenberg-Richter law colored for different low magnitude cutoff.
b) the same as a), but for b-positive.
c) b-value estimates for different low magnitude cutoff.
d) the same as c), but for b-positive.
e) probability of b-value and b-positive estimates.

100

a)

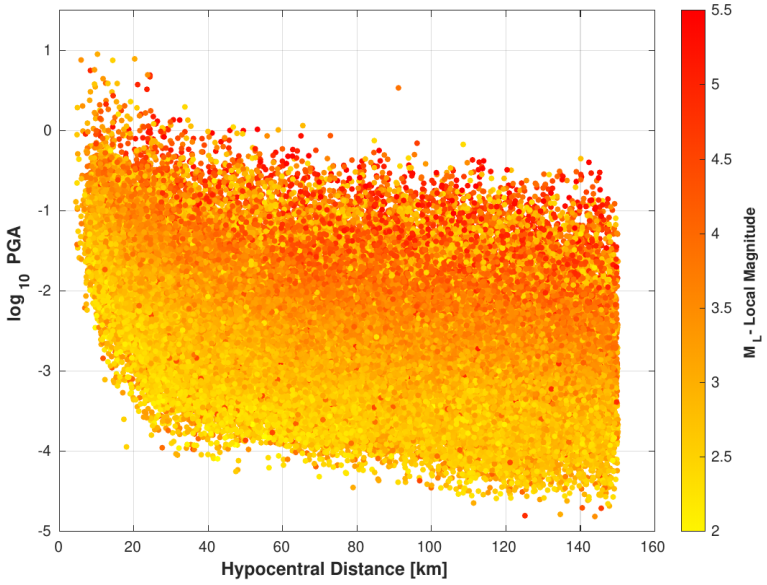

105

b)

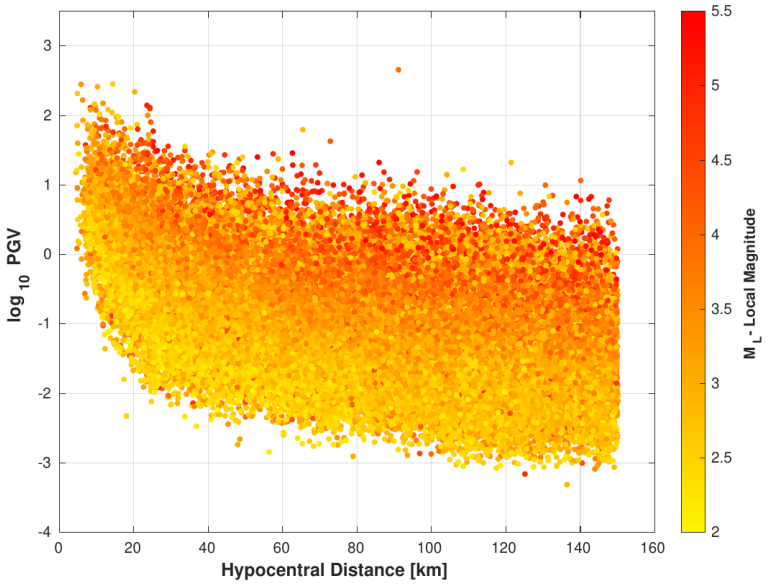

110

Figure S10: Distribution with hypocentral distance of the log10 PGA (a) and log10 PGV (b) over the S-wave time window. The color scale is proportional to the local magnitude M_L. PGA values are expressed in cm/s², PGV in cm/s.

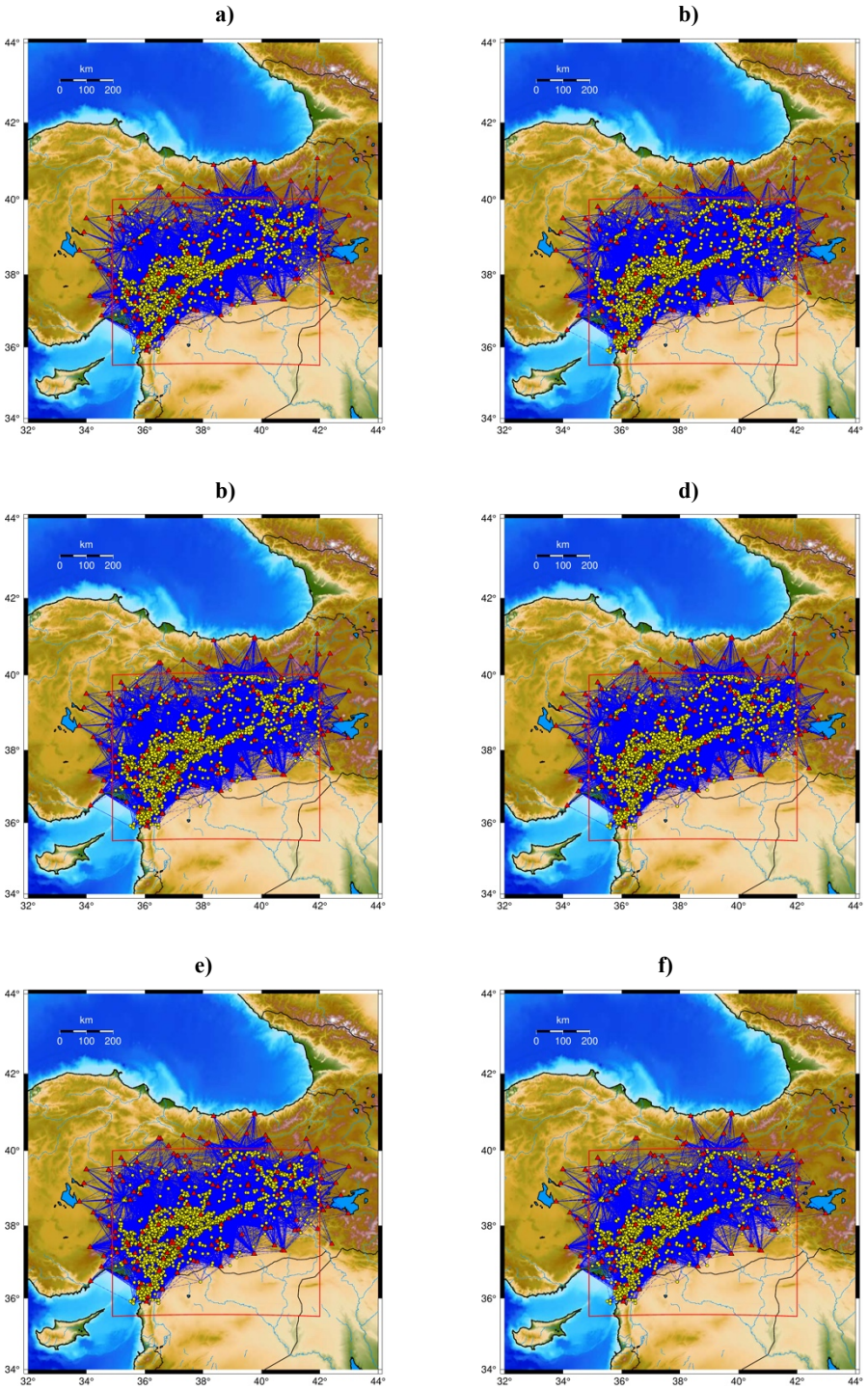

Figure S11: Ray coverage map at different frequencies: a) f=0.5 Hz; b) f=2 Hz; c) f=5 Hz; d) f=10 Hz; e) f=15 Hz; f=20 Hz. Events are shown by yellow dots, stations by red triangles and rays by blue lines.

130

a)

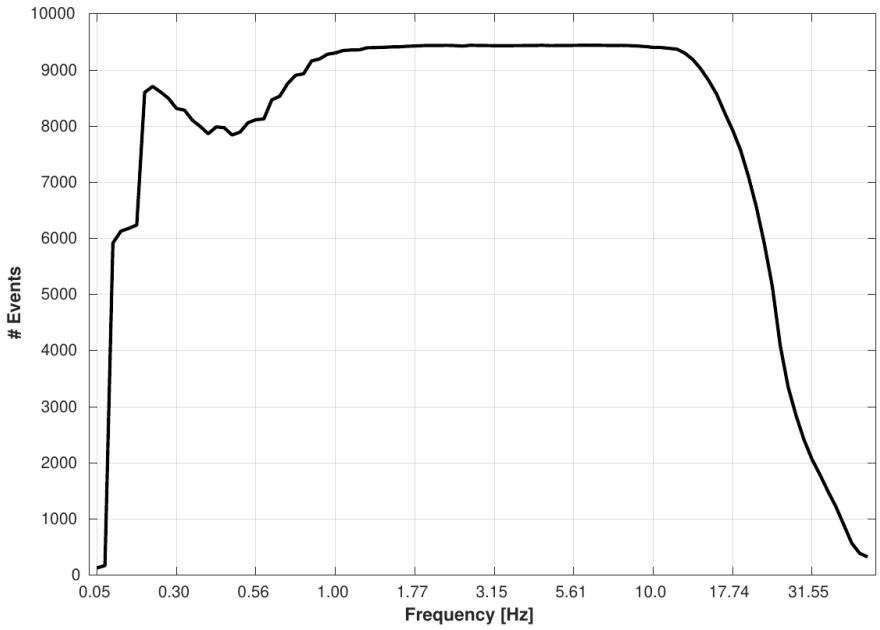

b)

135

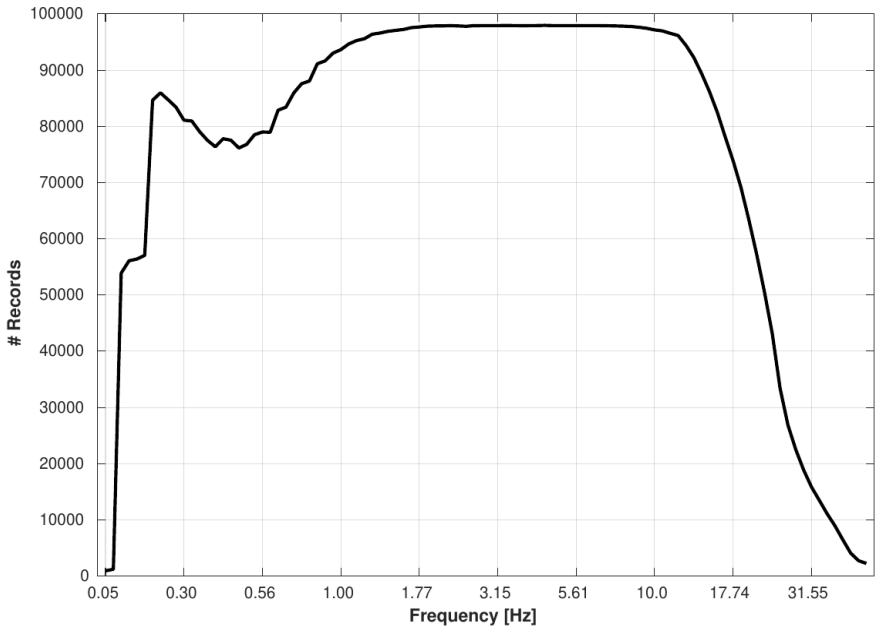

Figure S12: Number of events a) and records b) in function of frequency.

a)

b)

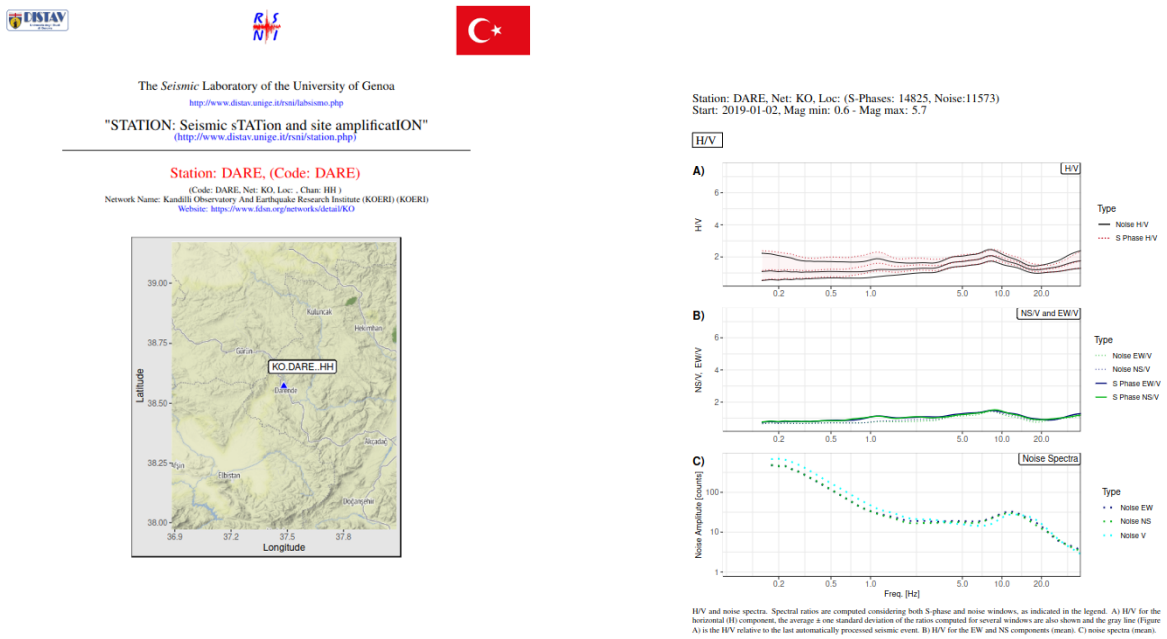

c)

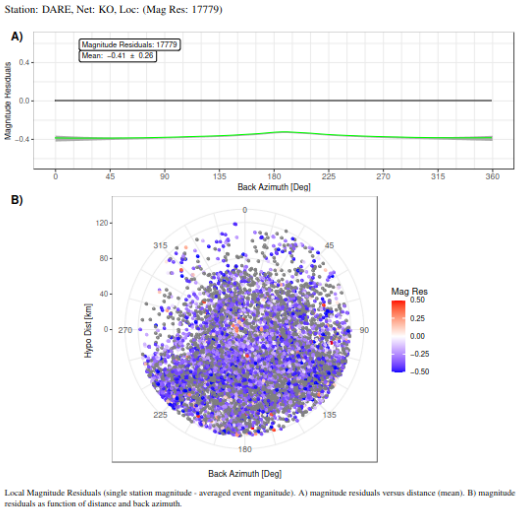

Figure S13: a) PDF document for the station DARE; b) HVSR measurements; c) Station Magnitude residuals and polar plot back-azimuth vs hypocentral distance.

a)

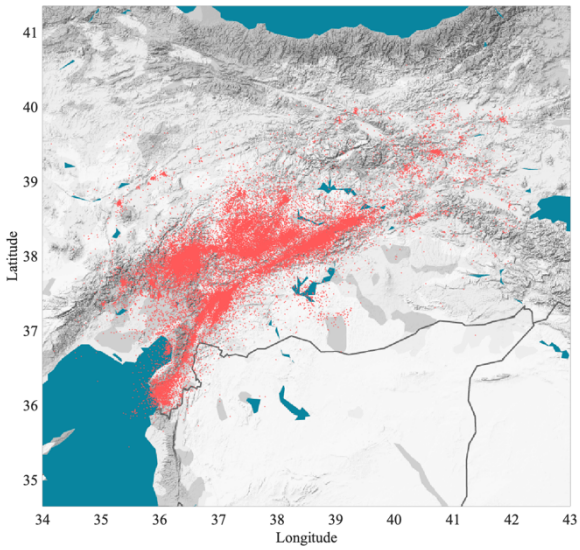

b)

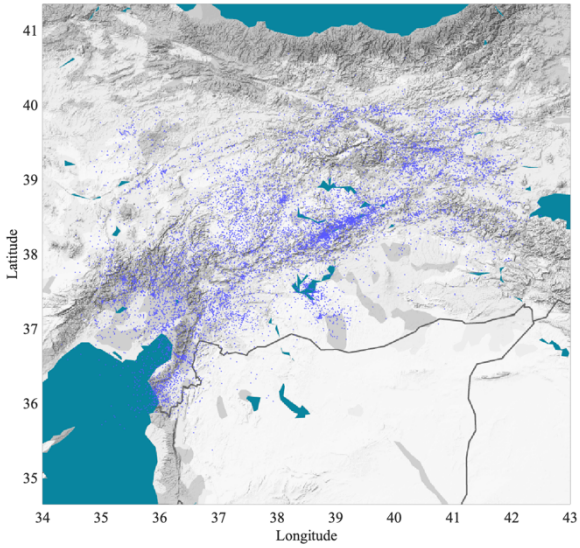

Figure S14: Map of clustered events (in red) and background events (in blue) of the study area.

Depth (km)	Vp (km/s)	Vs (km/s)
0	3.88	2.04
1	4.52	2.43
2	5.62	3.03
4	5.75	3.31
6	5.85	3.38
8	5.96	3.43
10	6.00	3.44
12	6.05	3.46
16	6.32	3.62
20	6.40	3.67
25	6.83	3.92
30	6.89	3.94
37	7.80	4.40
45	8.22	4.56
60	8.30	4.61

Table S1: 1-D velocity model used by Güvercin et al. (2022).

log(A_0) [mm]	Hypo. Dist. [km]
-1.07244174898789	1
-1.35966885608513	6
-1.7160981199827	12
-1.98892830272993	17
-2.13590773622714	21
-2.25363683689613	25
-2.35916366269252	29
-2.44766474104661	33
-2.53240943860632	37
-2.61021249040695	41
-2.66528693249829	45
-2.71432473016411	49
-2.76920664624866	53
-2.8191669249593	57
-2.86747402825801	61
-2.91830902407577	65
-2.94483049442765	69
-2.97215897437123	73
-2.99695095801442	77
-3.02269154981402	81
-3.05424871270596	85
-3.08327063753436	89
-3.09998195213348	93
-3.10103337983401	97
-3.1048308569975	101
-3.12338149725456	105
-3.14040055466825	109
-3.14893211133948	113
-3.16393664924174	117
-3.18257493288475	121
-3.19793731020898	125
-3.20847655774353	129
-3.22572956384246	133
-3.2403844942238	137
-3.25089747760466	141
-3.26015283312212	145
-3.27195727105306	150

Table S2: Table with the values of logA_0 versus hypocentral distance used for the calibration of local magnitude.